www.sciencetranslationalmedicine.org/cgi/content/full/5/200/200ra116/DC1

Supplementary Materials for

Up-Regulation of PD-L1, IDO, and T_{regs} in the Melanoma Tumor Microenvironment Is Driven by $CD8^+$ T Cells

Stefani Spranger, Robbert M. Spaapen, Yuanyuan Zha, Jason Williams, Yuru Meng, Thanh T. Ha, Thomas F. Gajewski*

*Corresponding author. E-mail: tgajewsk@medicine.bsd.uchicago.edu

Published 28 August 2013, *Sci. Transl. Med.* **5**, 200ra116 (2013)
DOI: 10.1126/scitranslmed.3006504

The PDF file includes:

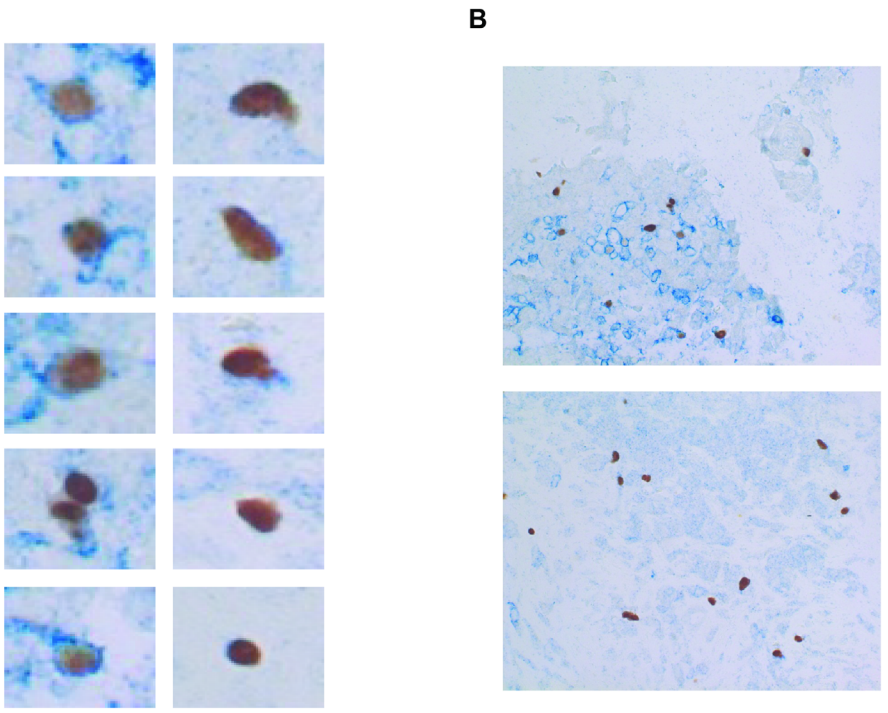

Suppl. Fig 1

Figure S1. Costaining of CD4 and FoxP3 in human melanoma sections. Immunohistochemistry staining for CD4 (blue) and FoxP3 (brown) in human melanoma tissue samples (400x). Left panel depicts zoom-in images out of the tumor shown on the right. All $FoxP3^{+}$ cells were identified to have detectable CD4 staining.

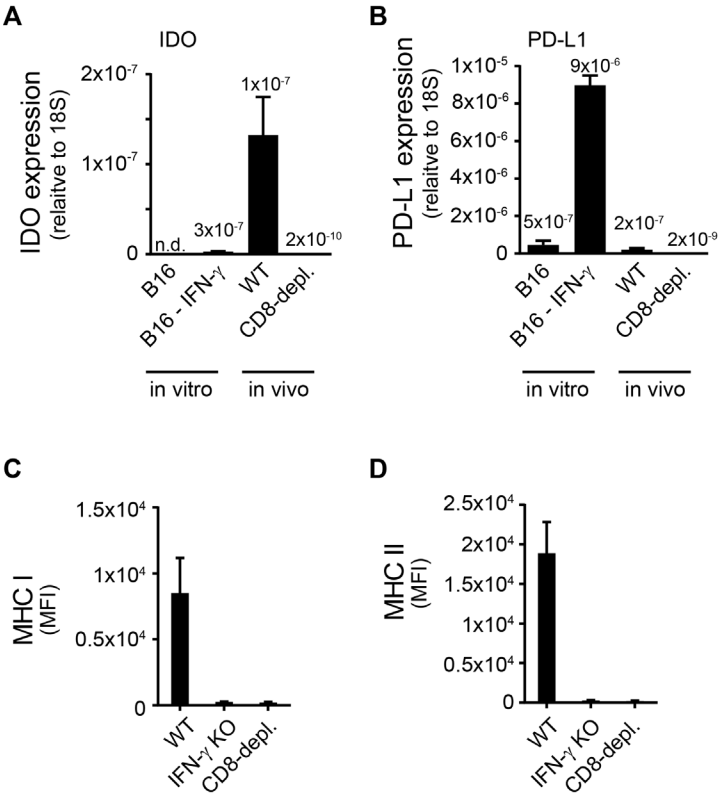

Suppl. Fig 2

Figure S2. Expression level of IDO, PD-L1, and MHC I/II in B16 tumors in vitro and in vivo. A-B. Quantitative RT-PCR for IDO and PD-L1 comparing parental B16 untreated (B16) or treated with IFN-γ (B16-IFN-γ) to in vivo injected B16 cell either into wild type mice (WT) or CD8-depleted mice (CD8-depl). C-D. Flow cytometric analysis of MHC-class I (C) and MHC-class II expression (D) assessed in B16-tumors transplanted either in wild type (WT), IFN-γ-knock out (IFN-γ-KO) or CD8-depleted mice (CD8-depl).

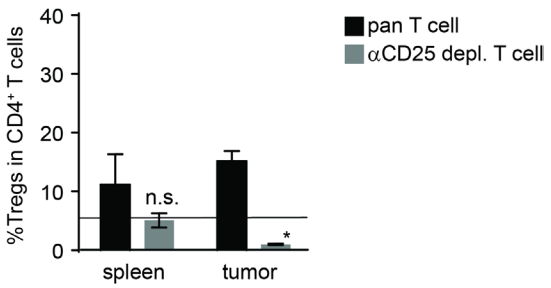

Suppl. Fig 3

Figure S3. Lack of T_{reg} conversion from CD25-depleted T cells. B16 tumors were engrafted into Rag2$^{-/-}$ mice (day 0) prior to transfer either pan T cells ($3x10^6$) or αCD25-depleted T cells ($3x10^6$) (day1). On day 7 spleen, tumor-draining lymph node and tumor were harvested and analyzed for the amount of FoxP3-positive CD4 T cells ($CD3^+$, $CD4^+$). Depicted are means with SEM of 3 mice each. Significance was tested with Mann-Whitney-U test with * = 0.03.

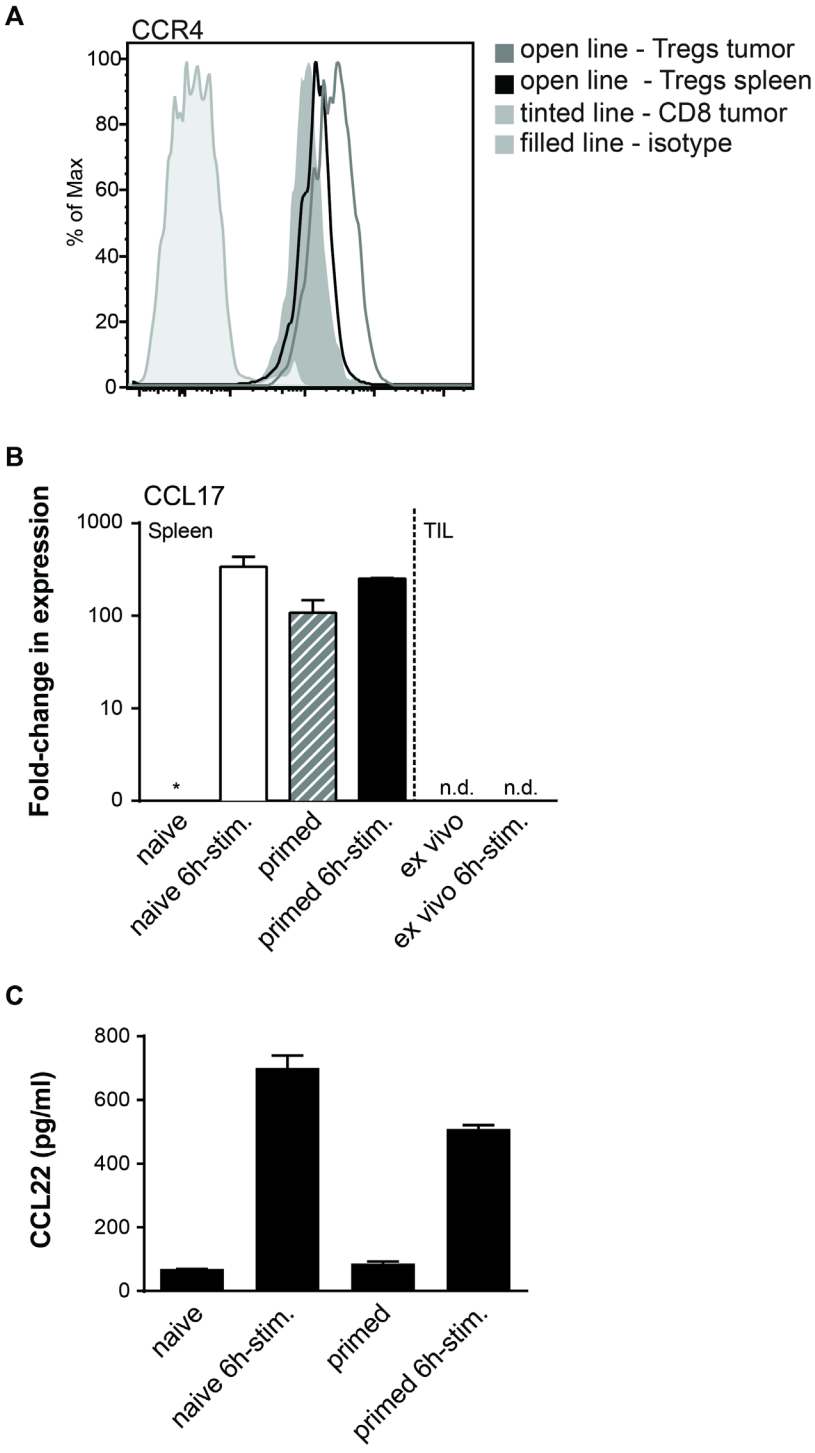

Suppl. Fig 4

Figure S4. Characterization of TILs compared to in vitro-primed CD8 T cells. A. CCR4 expression on Tregs, isolated from spleen (black open line) or tumor (grey open line), was compared to the expression on $CD8^+$ tumor-infiltrating lymphocytes (tinted line). B. Expression

of CCL17 in CD3/CD28-activated naïve $CD8^+CD62L^+$ lymphocytes was assessed using quantitative RT-PCR. Depicted is fold-change of 6h-activated, primed (7-day stimulation) and restimulated primed cells (primed 6h-stim) relative to naïve cells. Tumor-infiltrating $CD8^+$ T cells were isolated via fluorescence-activated cell sorting and analyzed for the expression of CCL17 with expression being below detection levels (n.d.). Data are shown in mean with SEM (n=3). C. Amount of secreted CCL22 was assessed using a CCL22-specific ELISA. Supernatants analyzed were harvested from non-stimulated cells (naïve) or CD3/CD28 stimulated cells (6h-stim) as well as 7-day stimulated cells (primed) and restimulated primed cells (primed 6h-stim). Depicted are means with SEM (n=2).

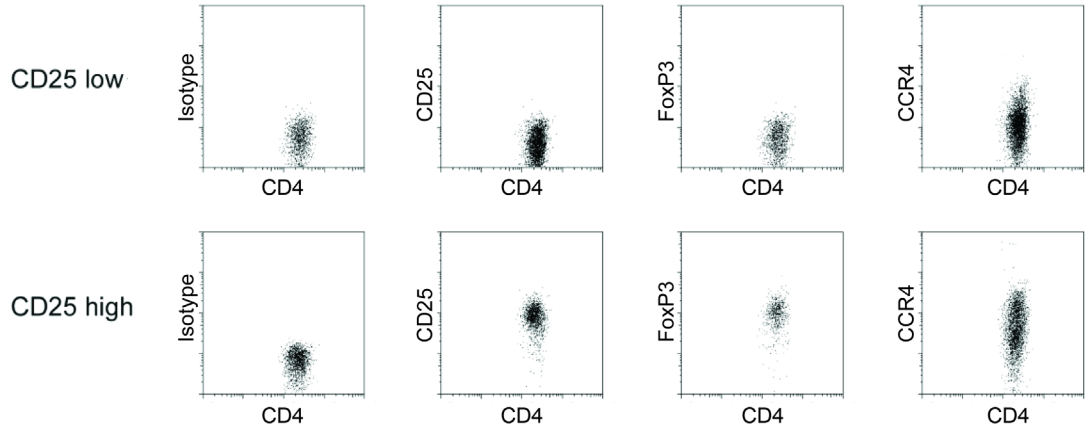

Figure S5. CCR4 expression on human CD4 T cells and T_{regs}. Human $CD25^{hi}CD4^+$ T cells express CCR4. Flow cytometry was performed using an anti-CCR4 mAb after flow cytometric sorting of $CD4^+CD25^+$ T cells from normal donor PBMCs.

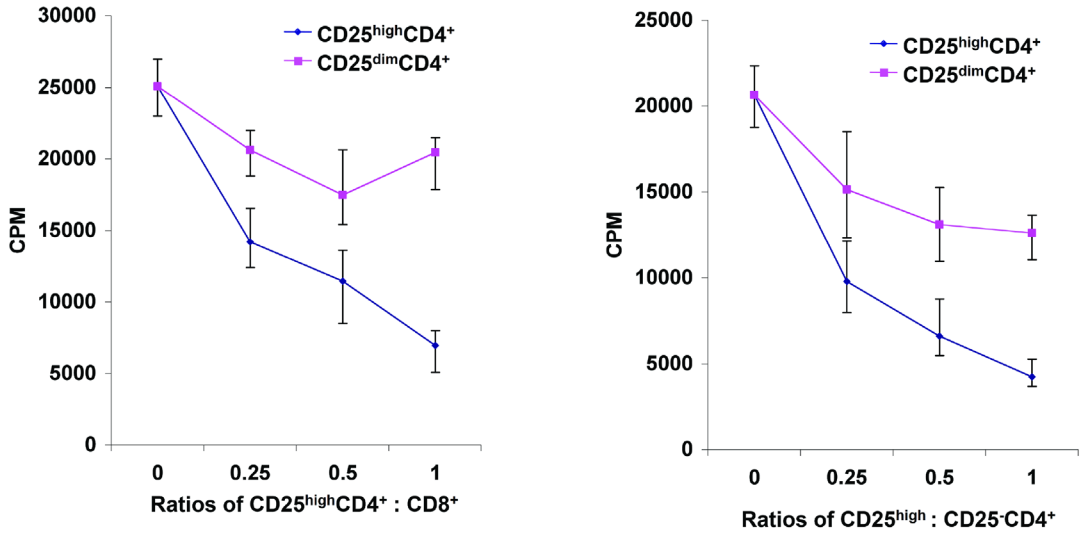

Suppl. Fig 6

Figure S6. Suppressive functional capacity of human CD25^{hi} T_{regs}. Human CD25^{hi}CD4^{+} T cells show suppressive function against CD4^{+} and CD8^{+} conventional T cells in vitro. Sorted CD25^{dim} cells are shown for comparison.